The International Journal of Advanced Manufacturing Technology (2025) 137:1565–1580
https://doi.org/10.1007/s00170-025-15231-5

ORIGINAL ARTICLE

An investigation of the curvature variation in rolling a stiffened panel

Yasir Alfawzan[1,2] · Jiaxin Lv[1,3] · Zhusheng Shi[1] · Jianguo Lin[1,4]

Received: 7 October 2024 / Accepted: 6 February 2025 / Published online: 22 February 2025

Abstract

Integral aluminium-stiffened panel, recognised for their light weight and superior performance, holds great potential for manufacturing through a combination of extrusion and subsequent rolling. Rolling these panels often leads to undesired curved shape due to their asymmetrical cross-sections; a careful control of rolling parameters for asymmetrical rolling is therefore essential to achieve the target shape—either straight or with specific curvature. The key influencing factors and their influencing mechanisms, however, have not been clarified. This study investigates the effects of various rolling parameters on panel curvature through finite element simulations. The results reveal that the primary influencing factors are plate thickness reduction, stiffener reduction, and speed ratio at a given geometry, while secondary factors include roll diameter, friction coefficient, temperature, roll speed, and panel material. Increasing the plate thickness reduction increases the curvature, while increasing the stiffener reduction reduces it. A higher speed ratio also decreases the curvature. Additionally, maintaining equal reductions in the plate thickness and stiffener can produce the most geometrically accurate panels, preventing material underfill or overfilling of the groove during rolling. The findings suggest that appropriate combination of rolling parameters enables the precise control over the curvature, contributing to the development of an efficient, high-performance rolling process for aluminium-stiffened panels.

Keywords Stiffened panel · Groove rolling · Asymmetrical rolling · Aluminium alloy · Finite element simulation

Nomenclatures

H_O, H (mm)	Plate thickness before and after rolling, respectively
h_o, h (mm)	Stiffener height before and after rolling, respectively
w (mm)	Width of plate
t_o, t (mm)	Bottom stiffener thickness before and after rolling, respectively
θ (°)	Stiffener slope angle
$A_{stif.0}$, $A_{stif.}$	Stiffener cross-section area before and after rolling, respectively
r_p, $r_{stif.}$ (%)	Reductions of plate thickness and stiffener, respectively
δ_r (-)	Reduction ratio = $r_{stif.}/r_p$
D_1, D_2, D_3 (mm)	Diameters of lower and upper rolls, and the groove, respectively
δ_D (-)	Diameter ratio D_2/D_1
ω_1 & ω_2 (rpm)	Angular speeds for lower and upper rolls, respectively
δ_ω (-)	Angular speed ratio ω_2/ω_1
μ_1, μ_2 (-)	Friction coefficients for lower and upper rolls, respectively
δ_μ (-)	Friction coefficient ratio μ_2/μ_1
R (mm)	Curvature radius
k (mm^{-1})	Curvature

✉ Jiaxin Lv
j.lv19@imperial.ac.uk

1 Department of Mechanical Engineering, Imperial College London, London SW7 2AZ, UK

2 King Abdulaziz City for Science and Technology (KACST), P.O. Box 6086, 11442 Riyadh, Saudi Arabia

3 Department of Mechanical Engineering, The Hong Kong Polytechnic University, Hung Hom, Kowloon, Hong Kong

4 Department of Industrial and Systems Engineering, The Hong Kong Polytechnic University, Hung Hom, Kowloon, Hong Kong

1 Introduction

Aluminium-stiffened panels, comprising wide aluminium plate with high-thin stiffeners, are commonly used in transportation, marine, and engineering structures owing to their ability to enhance load-carrying capacity while reducing overall weight [1, 2]. Traditional methods for manufacturing

the wide stiffened panels include welding, riveting, and machining, which present disadvantages in productivity, reliability, and cost due to the complexity of the manufacturing process [3, 4]. These methods also have drawback in performance and quality, for example, welding weakens the heat-affected zone [5], riveting adds weight [6, 7], and machining leads to material waste [8]. The integral structure of wide aluminium-stiffened panel has emerged as a promising trend in industries, offering reduced manufacturing costs without compromising structural weight and performance, while also minimising the number of parts and manufacturing time [9].

An integral stiffened panel can be manufactured through extrusion process [10], known for its ability to manufacture complex cross-sections. However, producing a high-quality and wide-thin stiffened panel through extrusion alone faces several critical limitations. Firstly, extruding wide-thin panels requires high extrusion force and significant energy consumption [11]; Secondly, achieving very thin plate thickness with high surface quality is challenging due to the increased probability of defects such as scratch, crack, and rough surfaces. To address these challenges, a post-extrusion rolling process presents a promising method for refining the extruded stiffened panel to achieve desired geometries, surface quality, and mechanical properties [12]. The integral extrusion-rolling process enhances the feasibility and efficiency of producing withthin and high-quality stiffened panels, optimising energy consumption and overcoming the limitations of extrusion alone. This innovative approach provides a superior alternative to traditional methods for manufacturing stiffened panels.

The rolling process of an extruded stiffened panel can be complex. A specially designed grooved roll is required so as to simultaneously form both the plate and stiffeners in the stiffened panel. Additionally, due to the asymmetric geometry of the stiffened panel's cross-section, conventional symmetric rolling in both diameter and speed is unsuitable as it would cause bending after rolling [13], meaning that further straightening operations or curvature modifications are necessary to obtain the final straight stiffened panels or a desired curvature profile. In this case, the asymmetric rolling (ASR) process could be a more attractive solution for directly producing straight stiffened panels or a desired profile due to its ability to adjust the curvature by differentiating the parameters between the upper and lower rolls [14]. The ASR can be realised via the difference in the rolling parameters between the upper and lower rolls, such as rotational speeds, diameters of rolls, coefficients of friction of roll surfaces [15, 16]. However, most studies on ASR are limited to the forming of flat plates, and applications of ASR in the rolling of stiffened panels are rarely seen.

The curvature of asymmetrically rolled (ASR) plates has been a subject of investigation for decades, with engineers exploring experimental, theoretical, and analytical approaches. The curvature varies with changes in plate thickness, plate thickness reduction, speed ratio, diameter ratio, and friction ratio [17, 18]. Specifically, curvature tends to align with faster roll [19], and with a higher speed ratio resulting in larger curvature [20]. However, Knight et al. [21] observed that while thicker plates tend to curve towards the faster roll, thinner plates may exhibit upward or downward curvature. Salimi et al. [22] similarly noted curvature tendencies towards the faster roll and higher friction roll at specific plate thickness reductions, but at higher reductions, the influence of these parameters on the curvature shape profile reduced. Contrasting viewpoints emerge in the literature, with Buxton et al. [23], suggesting that at high speed ratios, plates turn towards the slower roll, while at low speed ratios with low friction coefficients, plates may curve upwards or downwards [24]. Roll diameter and its ratio also play a role, with larger roll diameters yielding smaller curvature, and curvature tending towards the smaller diameter [25]. Jeswiet et al. [26] observed that at lower reductions, curvature decreases with increasing speed. However, as reduction increases, speed's influence on curvature diminishes, highlighting reduction's significant role in curvature magnitude and direction, becoming a dominant parameter in some cases. Curvature increases with an increase in the reduction of plate thickness, the speed ratio, and a decrease in the plate thickness [27]. Moreover, Collins et al. [28] found that the curvature may change in either direction with changing the reduction of the plate thickness and the diameter ratio. Plate thickness also exerts influence, with thicker plates yielding reduced curvature (flatter) but requiring increased force and torque, while thinner plates exhibit larger curvature [25, 27]. This disparity arises from the fact that the curvature is controlled by a variety of rolling parameters, prompting, researchers to explore combined factors like shape factor (the ratio of contact length to the mean thickness before and after rolling), and roll gap factor (the ratio of roll radius to initial thickness) [21, 29]. Despite these efforts, accurately predicting curvature trends remains challenging. Overall, the curvature phenomenon in ASR is complex due to many influencing parameters, including reduction of plate thickness, rotation speed and its ratio, roll diameter and its ratio, friction coefficient and its ratio, and plate thickness [30]. Changes in any of these variables can alter the plate's curvature, making prediction difficult. This complexity is even greater for rolling stiffened panels, as adding stiffeners further complicates curvature behaviour prediction.

In this paper, a comprehensive series of finite element (FE) simulations was conducted to analyse the curvature variation of the rolled stiffened panels under different rolling parameters, including speed ratio, reductions of both plate thickness and stiffener, rolling temperature, friction, roll diameter, and original stiffened panel geometries. The goal was to produce either a straight profile or a specific curvature by precisely adjusting the rolling parameters. This comprehensive simulation study provides valuable

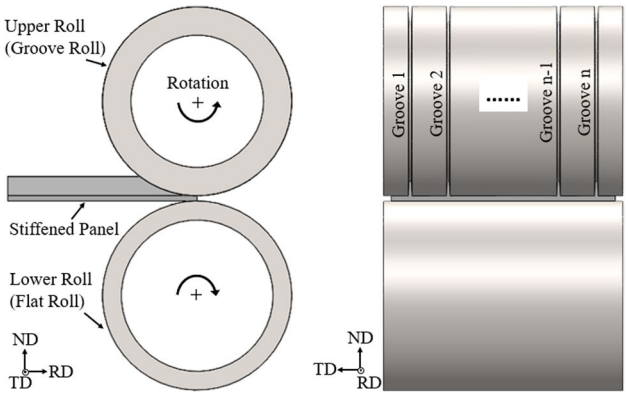

Fig. 1 Illustration of multi-groove rolling method, consisting of lower roll (flat roll), and upper roll (groove roll) as rolling tools, and stiffened panel as a workpiece

insights for optimising the rolling process to achieve high-quality stiffened panels with specific curvature characteristics, advancing the development of an innovative integral extrusion-rolling method for producing wide-thin stiffened panels.

2 Asymmetric groove rolling design and numerical modelling

2.1 Rolling method for panels with multiple and single stiffeners

Figure 1 illustrates a schematic of the multi-groove rolling method, consisting of a lower flat roll and an upper groove roll as rolling tools, with a stiffened panel as a workpiece. This method uses a pre-extruded stiffened panel and allows the rolling reduction on both stiffeners and the plate of the panel during the rolling process. In this study, all the stiffeners of the stiffened panel are identical. Therefore, the repeatable unit, i.e. a single-stiffener panel, is selected as the focus of the subsequent analysis.

Figure 2a shows the geometry of the original single-stiffened panel before rolling consisting of (1) a plate with a thickness H_o of 3 mm, and widths w_o range from 20 mm, 40 mm, 80 mm, to 160 mm, and (2) a stiffener with a height h_o ranges from 5 to 10 mm, a bottom thickness t_o of 1.9 mm, and a slope angle θ of 3 ° for different geometry cases. Figure 2b shows the geometry of the upper and lower rolls and the gap between them (rolling

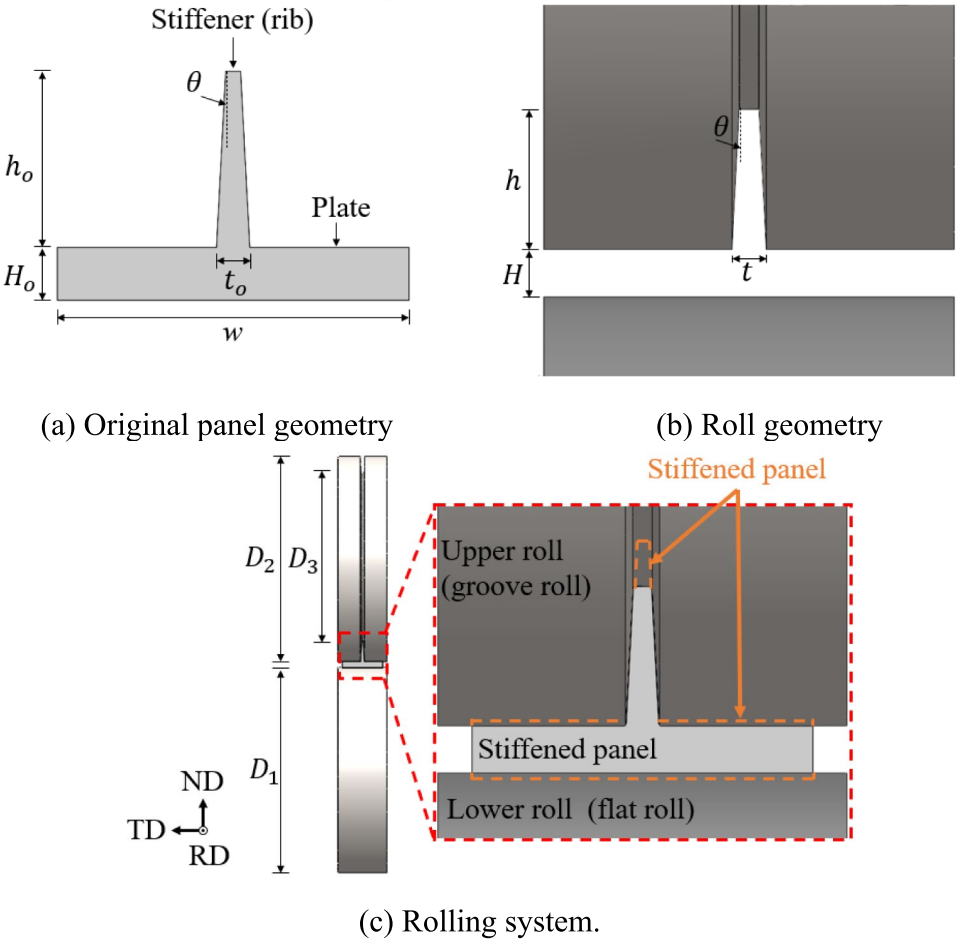

Fig. 2 Illustration of the geometry for rolling a single-stiffener panel. The hidden stiffened panel is highlighted with orange dashed lines (not to scale) for clarity

gap), which matches the final shape of stiffened panel after rolling. The rolling gap is represented by H, indicating the final plate thickness of the stiffened panel after rolling. The groove height is denoted by h, representing the final height of the stiffener, and the bottom thickness is referred to as t. The final slope angle of the stiffener remains unchanged. Figure 2c illustrates a schematic of rolling a single stiffened panel, featuring a lower roll (flat roll) with a diameter of D_1 ranges from 100 mm, 200 mm, to 400 mm, and an upper roll (groove roll) showing two diameters: the outer surface diameter D_2 ranges from 100 mm, 200 mm, to 400 mm, and the inner diameter for the top surface of the groove D_3 which defined by $D_3 = D_2 - 2h$. It also depicts an original stiffened panel positioned between the two rolls, ready for rolling. The shape of the hidden stiffened panel is depicted by orange dashed line.

2.2 Determination of roll design geometry

Various original and final panel geometries, including plate thicknesses and stiffener heights, have been analysed in this study. The roll design geometry, i.e. the dimensions, is determined by calculating the desired final dimensions of the panel after rolling, based on the initial panel geometry, and the targeted reductions in both plate thickness and stiffener.

The plate is rolled by passing it between two rolls to reduce its thickness, while the stiffener is rolled through a groove, experiencing both lateral deformation and deformation in the rolling direction. This dual deformation reduces the stiffener's height while allowing it to expand laterally to fill the final groove dimensions. The groove on the upper roll was designed to be 5% wider than the original stiffener thickness to prevent overfilling during the rolling process. This choice aligns with roll pass design principles in similar studies, which recommend slight oversizing to ensure proper material flow without inducing stress concentrations or shape inaccuracies [31, 32]. The 5% increase provides sufficient space for lateral deformation while maintaining adequate contact between the stiffener and the groove, thereby improving the final geometry's accuracy and preventing defects. The final dimension of the groove thickness is calculated as:

$$t = 1.05 \times t_o \tag{1}$$

Two assumptions have been applied during the calculation. Firstly, the volume of the stiffened panel is assumed constant before and after rolling, and any change in volume due to closing of voids in the extruded panel after rolling is neglected. Additionally, it is assumed that there is no lateral spread during the rolling process for the plate, meaning the plate's width remains constant before and after rolling. This assumption is based on the premise that the width to rolling contact length ratio is high enough to prevent lateral spread [33], which ensures that deformation flow occurs only within the rolling direction. The following paragraphs detail the calculating process under various reduction scenarios.

To ensure that no plastic instability or material tearing occurring, the model was carefully designed to avoid any damage to both the stiffener and the plate. This included maintaining a similar shape of the stiffener cross-section before and after rolling, applying a similar range of reduction for both the plate and stiffener, designing the stiffener with an inclination, and adding fillets at the edges to facilitate smoother deformation flow.

According to the definition of the plate thickness reduction r_p, i.e. the ratio of the difference between the plate thickness before and after rolling to the original plate thickness, the plate thickness after rolling H can be calculated as:

$$H = H_0 \times (1 - \frac{r_p}{100\%}) \tag{2}$$

Given an original plate thickness $H_0 = 3$ mm, and three different plate thickness reductions r_p= 5%, 10%, and 15%, the calculated plate thicknesses H would be 2.85 mm, 2.7 mm, and 2.65 mm, respectively as shown in Table 1.

On the other hand, the stiffener will experience deformation flow within rolling direction and lateral direction due to its hight and thinness as shown in Fig. 2, and because the groove is wider than the original stiffener thickness, which means the stiffener reduction cannot be defined by the reduction on the stiffener height only because it will experience a change in its height and thickness of its cross-section area. Therefore, stiffener reduction r_{stif} represents the ratio of the difference in its cross-sectional area before and after rolling to the cross-sectional area before rolling, i.e.

$$r_{stif} = \frac{A_{stif.0} - A_{stif}}{A_{stif.0}} \times 100\% \tag{3}$$

where $A_{stif,0}$, and A_{stif} are the cross-sectional areas for the stiffener before and after rolling, respectively. These can be calculated as:

$$A_{stif.0} = \left(h_0 \times t_o\right) - \left(tan\theta \times h_0\right) \times h_0 \tag{4}$$

$$A_{stif} = (h \times t) - (tan\theta \times h) \times h \tag{5}$$

The stiffener reduction can be formulated from Eqs. (2, 3, 4, and 5) as follows:

Table 1 Calculated final plate thickness at different r_p when H_0 = 3 mm

r_p(%)	H(mm)
5	2.85
10	2.7
15	2.65

$$r_{stif} = \frac{((t_o \times h_o) - (tan\theta \times h_o^2)) - (((1.05 \times t_o) \times h) - (tan\theta \times h^2))}{((t_o \times h_o) - (tan\theta \times h_o^2))} \times 100\% \quad (6)$$

For given two cases of original stiffeners height at h_0= 5 mm, or 10 mm, original thickness t_o= 1.9 mm, slope angle θ= 3 °, and final thickness t= 2 mm, and applying different stiffener reductions $r_{stif.}$= 0%, 2.5%, 5%, 10%, 15%, and 20%. The stiffener height will be changed according to its applied reduction value and its original height. The stiffener reduction can be formulated as follows:

$$r_{stif} = \frac{((1.9 \times h_o) - (h_o^2 \times tan3)) - ((2h) - (h^2 \times tan3))}{((1.9 \times h_o) - (h_o^2 \times tan3))} \times 100\% \quad (7)$$

The stiffener height after rolling h will range from 6.65 to 9 mm for h_0= 10 mm and will range from 3.62 to 4.66 mm for h_0= 5 mm as shown in Table 2. All the dimensions of stiffened panel before and after rolling are summarised in Table 3. For changes in the height or inclination angle of the stiffener, a new groove design for the upper roll is required to ensure appropriate contact and deformation.

2.3 Numerical modelling

Numerical simulations were conducted using the finite element software QForm to explore the effects of various rolling parameters on the rolling behaviour, specifically on the curvature profile. The finite element (FE) model comprises a lower flat roll, and an upper groove roll, each with diameters ranging from 100 to 400 mm. Additionally, small guidance rolls with diameters of 10 mm were included, allowing for free rotation, and operating under frictionless conditions to guide the stiffened panel during entry. The rolls were made of H13 material. The stiffened panel materials investigated were AA1050 and AA6061, each with a plate thickness of 3 mm. The bottom stiffener thickness was 1.9 mm, with a 3° slope angle and 0.2 mm fillet at the edges. The length of both plate and stiffener is 100 mm. The front end of the stiffened panel was chamfered, and the panel was positioned to make slight contact with the rolling rolls for easy entry and pulling. A schematic of the model setup for a stiffened panel with a single stiffener, along with the application of a symmetry plane on the RD-ND plane to reduce computational complexity, is depicted in Fig. 3. Various geometrical configurations and rolling conditions were considered, as outlined in Table 4, which includes the type of material used, rolling temperature, rolling reductions, rolling speed, roll diameter, and friction coefficient. The primary rolling conditions employed across most cases involve AA6061 material, a temperature T of 450 ℃, plate thickness H of 3 mm, stiffener height h of 10 mm, identical roll diameters D_1=D_2 = 100 mm, friction coefficients μ_1=μ_2= 0.8, and roll speed ω_1= 7.5 rpm, with a plate thickness reduction r_p=10%. Any deviations from these parameters are explicitly indicated in the figure captions. The rationale behind fixing most parameters while selectively altering one for study purposes is to ensure consistency and isolate the effect of the varied parameter.

Table 2 Calculated final stiffener heights at different r_{stif} and h_o

r_{stif}(%)	h(mm)	
	For h_o= 10 mm	For h_o= 5 mm
0	9	4.66
2.5	8.65	4.52
5	8.45	4.4
10	7.75	4.13
15	7.2	3.7
20	6.65	3.62

Table 3 Geometries and dimensions of the original and final stiffened panels. Final values of H and h are obtained at different r_p, and $r_{stif.}$ values respectively

Dimensions	Original value	Final value	
t(mm)	1.9		2
w(mm)	20		20
	40		40
	80		80
	160		160
θ(°)	3°		3°
H(mm)	3	r_p= 5%	2.85
		r_p= 10%	2.7
		r_p= 15%	2.65
h(mm)	10	$r_{stif.}$= 0%	9
		$r_{stif.}$= 2.5%	8.65
		$r_{stif.}$= 5%	8.45
		$r_{stif.}$= 10%	7.75
		$r_{stif.}$= 15%	7.2
		$r_{stif.}$= 20%	6.65
	5	$r_{stif.}$= 0%	4.66
		$r_{stif.}$= 2.5%	4.52
		$r_{stif.}$= 5%	4.4
		$r_{stif.}$= 10%	4.13
		$r_{stif.}$= 15%	3.7
		$r_{stif.}$= 20%	3.62

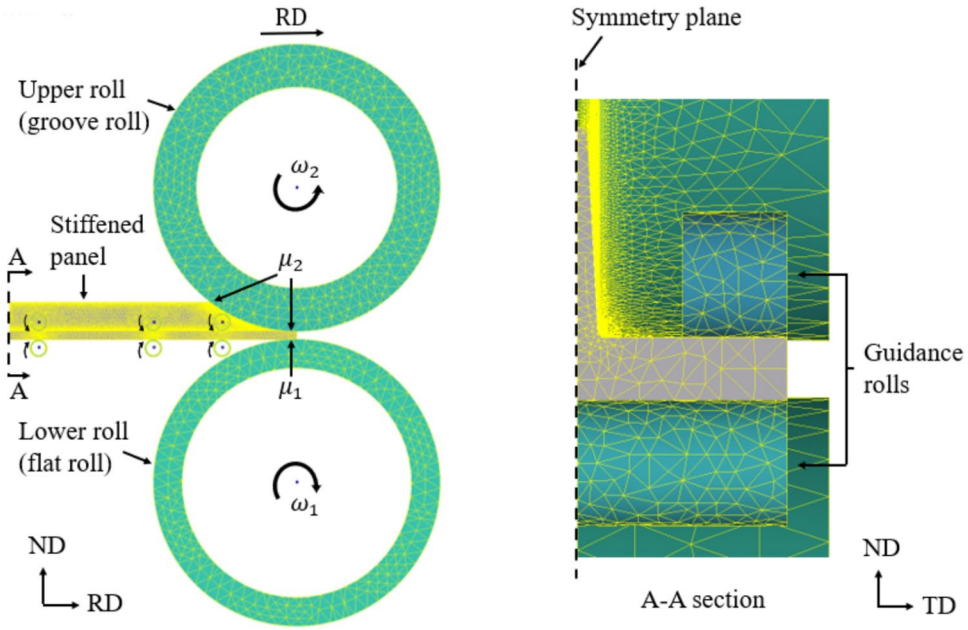

Fig. 3 FE model setup

Table 4 Rolling conditions in FE simulations

Geometries and parameters	Symbol	Value
Stiffened panel material	-	AA1050, AA6061
Rolls' material		H13
Rolling temperature (°C)	T	20, 360, 450
Plate thickness reduction (%)	r_p	5, 10, 15
Stiffener reduction (%)	$r_{Stif.}$	0, 2.5, 5, 10, 15, 20
Lower rotation speed (rpm)	ω_1	7.5, 15, 30
Speed ratio (-)	$\delta_\omega = \frac{\omega_2}{\omega_1}$	1, 1.11, 1.22, 1.33, 2
Lower, and upper rolls diameter (mm)	D_1,D_2	100, 200, 400
Roll diameter ratio (-)	$\delta_D = \frac{D_2}{D_1}$	100/100, 200/200, 400/400
Friction coefficient for lower, and upper rolls (-)	μ_1,μ_2	0.45, 0.8
Friction ratio (δ_μ)	$\delta_\mu = \frac{\mu_2}{\mu_1}$	0.4/0.8, 0.4/0.4, 0.8/0.8. 0.8/0.4

The Lagrangian method was employed for simulations within the QForm software environment. Material properties for both the workpiece (stiffened panel) and the tools (rolls) were specified using the standard database provided by QForm. Tetrahedral mesh elements were utilised, with automatic mesh size generation applied to both the tools and workpiece. Re-meshing of the workpiece occurred during the simulation, with a maximum of 20 steps between remeshings. The minimum and maximum adaptations in the workpiece were set to 1 and 15, respectively, with an adaptation factor of 1. Friction between the deformable workpiece and the tools was modelled using the Levanov friction model shear stresses as described in the Eq. 8 [34]:

$$\tau = \mu \times \frac{\sigma_T}{\sqrt{3}} \times (1 - e^{-n \times \frac{\sigma_n}{\sigma_T}}) \tag{8}$$

where τ is the Levanov friction model shear stresses, μ is a friction coefficient, σ_T is a flow stress, σ_n is a normal contact pressure, and n is a Levanov coefficient with a value of 1.25 as it is assumed by QForm database. The heat transfer coefficient used is 40 $kW/m^2.K$. The stop conditions are designed to halt the rolling simulation once the stiffened panel has advanced approximately 78.5 mm in the rolling direction.

3 Simulation results and discussion

3.1 Curvature *k*

This section elaborates on the calculation methodology employed to quantify and define the curvature, including the determination of curvature radius R and curvature k. The

curvature of the stiffened panel is quantified by computing the reciprocal of the curvature radius using the following formula:

$$k = 1/R \tag{9}$$

where R represents the curvature radius, calculated by identifying three points on the rolled stiffened panel after the rolling process, ensuring equal spacing between consecutive points. These known points, denoted as (x_1, y_1), (x_2, y_2), and (x_3, y_3), are then used to compute the radius of the arc passing through them [21]. To determine the curvature radius, the circle equation in general form, represented by Eq. (10), is employed [35]:

$$x^2 + y^2 + 2ax + 2by + c = 0 \tag{10}$$

where the a, b, and c are constant, in which a and b represent the centre of the circle, and R is the radius of this circle which represent curvature radius. By substituting the coordinates of the three known points into this equation, a system of three equations is formed and solved using matrix methods. Upon solving this matrix, the constants a, b, and c are determined. Subsequently, the curvature k can be calculated as follows:

$$k = 1/R = 1/\sqrt{a^2 + b^2 - c} \tag{11}$$

The curvature k serves as a descriptor of the stiffened panel's curvature profile. Values close to zero indicate a nearly straight panel, while positive and negative signs denote upward and downward curvature, respectively. These directional indications (signs) are later added based on the profile shape to provide a directional evaluation of the curvature profile.

3.2 Validation of the numerical model

The experimental rolling process for the AA6061 stiffened panel, conducted with a 15% plate thickness reduction, 10% stiffener reduction, and a speed ratio of 1.11, was performed to validate the simulation results. Figure 4 shows the photo after rolling and the comparison from side views between the physically rolled panel and the simulated rolled panel under the same rolling condition. The curvature radius and curvature for the experimental stiffened panel were approximately 128 mm and 0.0078 mm^{-1}, respectively, compared to 120 mm and 0.0083 mm^{-1} for the simulated stiffened panel. The percentage deviation between the experimental and simulated curvature radii was 6.25%, providing confidence in the FE model's reliability and ability to predict the effects of rolling parameters on curvature profiles.

3.3 Curvature variation with speed ratios and stiffener reductions

Figure 5 explores the evolution of curvature of stiffened panels with increasing speed ratio from 1 to 2 under varying stiffener reductions. At a constant stiffener reduction, the curvature k decreases with increasing speed ratio from 1 to 2, reaching the minimum at δ_ω =1.33, and then slightly increase with further increasing δ_ω. At a constant speed ratio, increasing stiffener reduction leads to the decrease in k, except for the case at $r_{stif.}$ of 0% and speed ratio of 1. In addition, at $r_{stif.}$ of 0% and 2.5%, all the k values are positive within the studied speed ratio region. For other $r_{stif.}$, k decreases from positive to negative with increasing speed ratio. For example, when the speed ratio transitions from 1.11 to 1.33 at a given plate thickness reduction of 10% and a stiffener reduction of 10%, the curvature undergoes

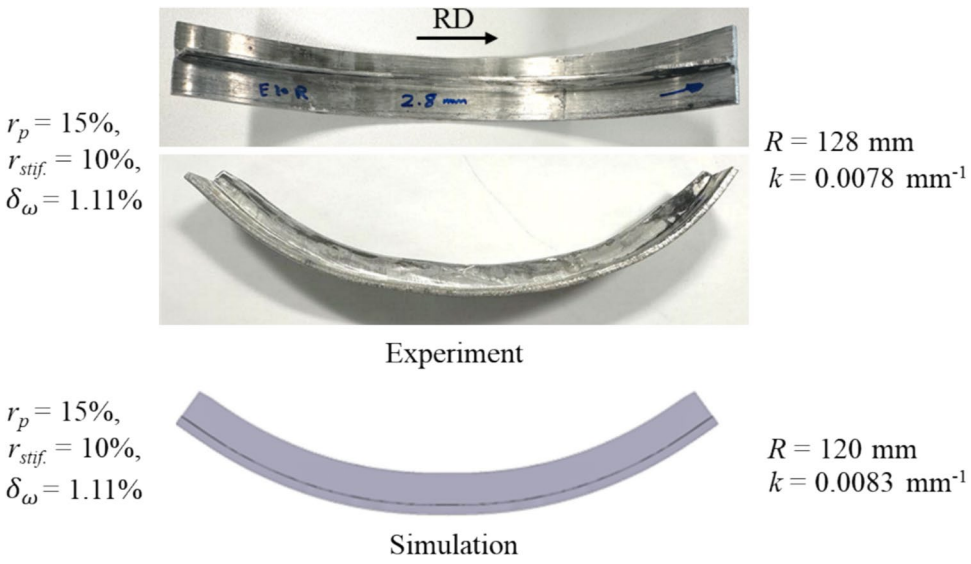

Fig. 4 Pictures of rolled AA6061 stiffened panels from rolling experiment and simulation, demonstrating the good agreement in curvature between the two profiles. The rolling conditions were a 15% plate thickness reduction, 10% stiffener reduction, and 1.11 speed ratio. RD represents the rolling direction

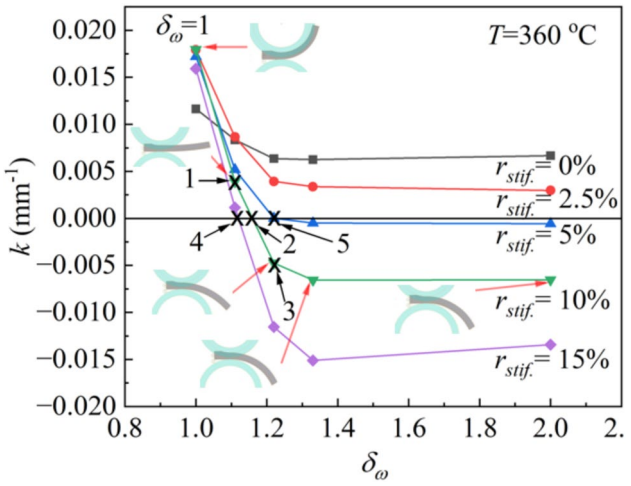

Fig. 5 The relationship between the curvature k and rotation speed ratio δ_ω at various stiffener reductions ranging from 0−15%. Five cases namely 1, 2, 3, 4, and 5 are marked with X shapes. The invariant rolling conditions are AA6061, T = 360 ℃, H_o = 3 mm, h_o = 10 mm, r_p = 10%, D_1 = D_2= 100 mm, μ_1 = μ_2 =0.8, ω_1 = 7.5 rpm. The simulation results of rolling curvature shapes at various conditions are depicted and indicated by red arrows

significant decrease from 0.004 to − 0.00656 mm^{-1}. This indicates there exist a specific point where the straight panel can be rolled, i.e. k =0 mm^{-1}, using an appropriated combination of rolling parameters specifically, the reductions of plate and stiffener, and the speed ratio.

Figure 6 illustrates the resulting curved variation, including upward, almost straight, and downward curves, observed in three different cases, namely 1, 2, and 3, as marked in Fig. 5. Through simulations, it becomes evident that achieving a straight stiffened panel is feasible across a range of rolling parameters, however, determine the exact values remains challenging. Notably, the curvature radius exhibits high sensitivity to changes in speed ratio, with even a small adjustment in speed ratio, changes the curvature radius dramatically. For instance, as the speed ratio transitions from 1.11, 1.13 to 1.22, the curvature radius undergoes significant changes, ranging from 256 mm, 1027 mm to − 211 mm (the negative sign was added to distinguish the downward curve), respectively. Within this range of speed ratio, the most optimal straight stiffened panel is achieved at a speed ratio of 1.13, wherein the highest absolute curvature radius of 1027 mm is attained. This range was systematically explored by incrementally adjusting the speed ratio from 1.11 to 1.22 by increments of 0.01. Although achieving a perfectly "straight" stiffened panel (i.e. k = 0 mm^{-1}) was not possible in the simulation, a sufficiently low absolute value of the curvature k can be considered acceptable for straight rolling, especially when followed by subsequent stretching in industrial practice.

3.4 Metal flow behaviour

Figure 7 shows the material deformation flow in the region between the stiffener and the plate during the rolling process for the three cases 5, 2, and 4 as marked in Fig. 5. These cases feature three stiffened panels which rolled at different stiffener reductions of 5%, 10%, and 15% with different speed ratios of 1.22, 1.13, and 1.11, respectively. The speed ratios were changed by 0.01 till reaching the minimum absolute value of k (near straight panel). The purpose of studying these cases is to analysis the effect of change the stiffener reduction at similar curvature profile. This visualisation is achieved by tracking the movement of a selected point (shown in black) originally positioned on the edge of

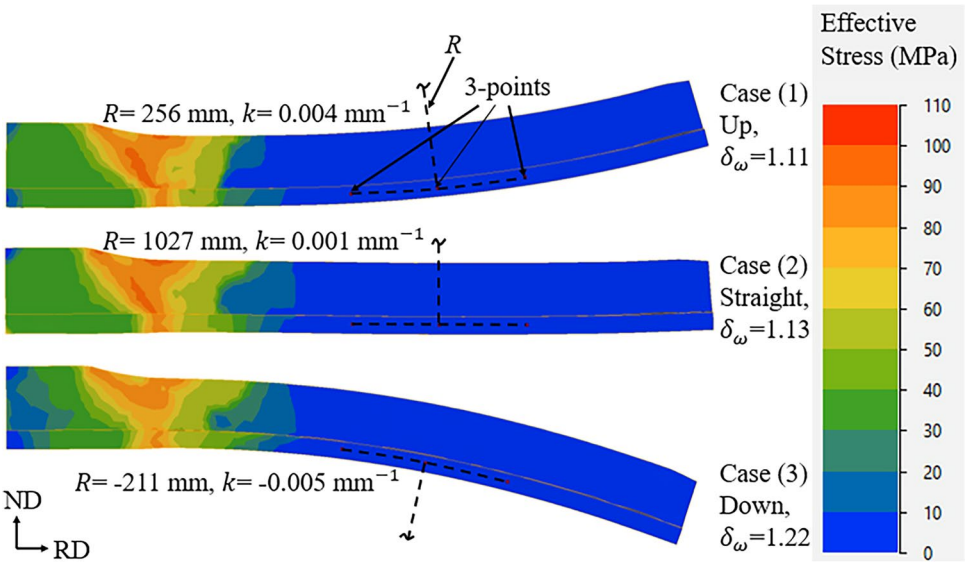

Fig. 6 Variation of curvature of three cases (1, 2, and 3) for three different speed ratios δ_ω = 1.11, 1.13, & 1.22. The rolling conditions are AA6061, T = 360 ℃, h_o = 10 mm, r_p = 10%, $r_{stif.}$= 10%, D_1 = D_2= 100 mm, μ_1 = μ_2= 0.8, ω_1= 7.5 rpm

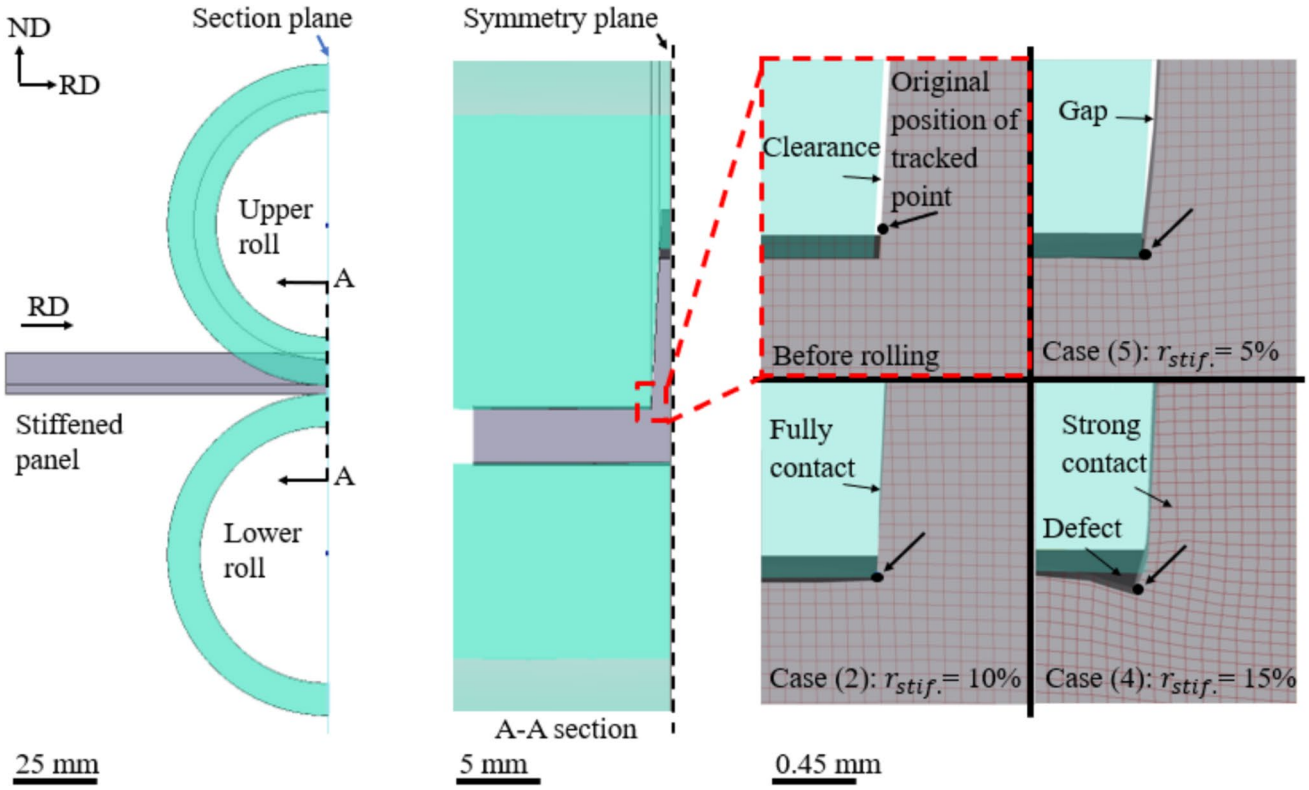

Fig. 7 Material deformation flow during rolling process for cases 5, 2, and 4. A black point, positioned in this area between the stiffener and the plate, is tracked to illustrate the flow pattern

stiffener during the rolling process. In case 4, the black point moves from the stiffener to the plate and accumulates under the upper roll (groove roll), resulting in minor defect in the edge between the stiffener and the plate. This occurrence stems from an excessive reduction in the stiffener, causing an overfill of the groove with material. Consequently, some of the material flows significantly from the stiffener to the plate during deformation, leading to slight distortion between the stiffener and the plate.

In cases 5 and 2, the black point moves a shorter distance due to a lesser reduction in the stiffener. In case 5, the gap clearance between the groove roll and the stiffener is not filled, resulting in incomplete contact on the stiffener surface, indicating insufficient reduction. Conversely, in case 2, full contact surfaces between the stiffener and the groove roll occurs, but not reach to overflow or overfill. However, this strong contact may increase friction between the groove roll and the stiffener surfaces, potentially leading to sticking between them. Therefore, lubricating the groove may be necessary to reduce these issues.

3.5 Mechanical analysis

Figure 8 illustrates the distribution of effective stresses on the cross-sections for cases 5, 2, and 4 (as marked in Fig. 5), where near-straight panels were obtained at stiffener reductions of 5%, 10%, and 15%, respectively, with corresponding speed ratios of 1.22, 1.13, and 1.11, respectively. Both the plate and stiffener exhibit non-uniform stress distribution across their cross sections. The maximum stress appears at the top part of the stiffener since plastic deformation from the stiffener height reduction concentrates in this region. This stress increases with greater stiffener reduction, as seen when comparing cases 5, 2, and 4. In addition, the minimum stress is observed at the bottom of the stiffener in case 5 due to limited deformation constraints from the rolls. However, as the stiffener reduction increases to 10% in case 2 and 15% in case 4, the stress at the bottom of stiffener also rises, attributed to the stronger contact between the stiffener material and the roll surface.

In case 4, which involves the largest stiffener reduction of 15%, the maximum effective stress reaches 96 MPa at the top of the stiffener. Additionally, the region between the stiffener and the plate shows elevated stress levels compared to the other cases, likely due to overfilling of the groove roll with material, leading to further compression stress. Conversely, case 5 experiences the lowest effective stress, with a maximum value of 81 MPa. This is attributed to the lower stiffener reduction of 5%, which leaves the groove unfilled, creating a gap between the deformed stiffener and

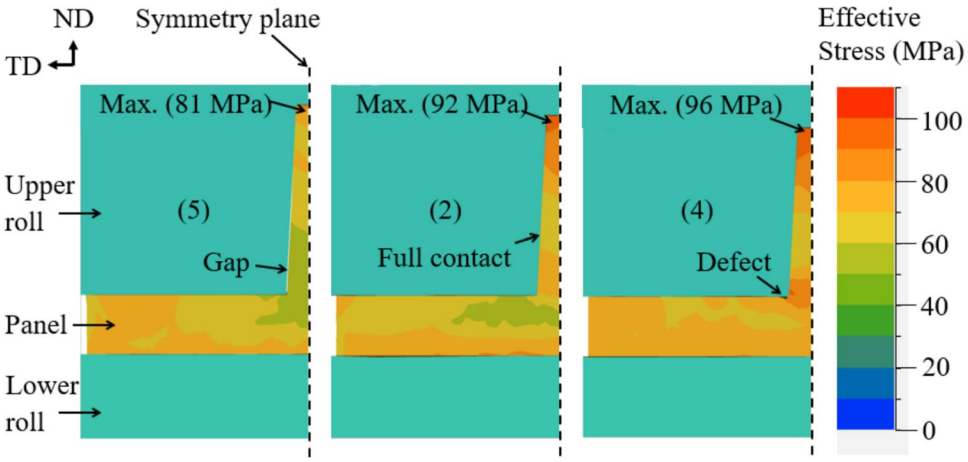

Fig. 8 Stress distribution on the cross-section of panels being rolled, under three different set of rolling parameters namely case 5 (at $r_{stif.}$ = 5%, & δ_ω= 1.22), 2 (at $r_{stif.}$= 10%, & δ_ω= 1.13), and 4 (at $r_{stif.}$= 15%, & δ_ω= 1.11)

the groove surface. As a result, the area between the plate and the stiffener experiences lower effective stress. Case 2 falls in between the two cases, experiencing full contact between the stiffener and groove roll surfaces.

3.6 Effect of various parameters on the curvature of rolled panel

The curvature variation results presented in this section are derived from an exhaustive analysis comprising 265 simulation cases under various rolling conditions, encompassing variations in plate thickness reductions, rolling temperatures, friction coefficients, rolling speeds, roll diameters, stiffener heights, plate widths, and materials.

This analysis of the curvature variation was represented by the variation of the curvature k of a rolled stiffened panel on the y-axis with different speed ratios δ_ω on the x-axis at different cases of rolling conditions and geometries as shown in Figs. 9, 10, 11, 12, 13, 14, 15, and 16 in the following subsections.

a) Plate thickness reductions $\boldsymbol{r_p}$

Figure 9 illustrates the variation of the curvature k as speed ratios δ_ω increase from 1 to 2, under different stiffener reductions $r_{stif.}$ of 5% and 10%, and plate thickness reductions r_p of 5%, 10%, and 15%. At a constant speed ratio and stiffener reduction, increasing the plate thickness reduction leads to an increase in k. For instance, at 1.22 speed ratio and 10% stiffener reduction, increasing the plate thickness reduction from 5 to 15% increased the curvature from − 0.01022 to 0.00178 mm^{-1}. This is likely due to the extended plate length relative to the stiffener length, inducing residual and bending stresses (tensile stress in the plate and compressive stress in the stiffener), which causes the

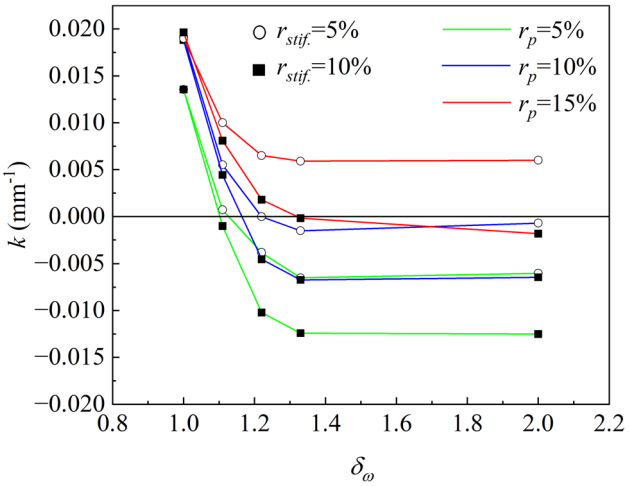

Fig. 9 The relationship between the curvature k and rotation speed ratio δ_ω at various stiffener reductions of 5% and 10%, for the plate thickness reduction of 5%, 10%, and 15%. The invariant rolling conditions are AA6061, T= 450 ℃, H_o= 3 mm, h_o= 10 mm, D_1=D_2= 100 mm, μ_1=μ_2= 0.8, ω_1= 7.5 rpm

panel to bend upward. Additionally, increasing the stiffener reduction from 5 to 10% lowers the curvature k for a given speed ratio and plate thickness reduction. At 1.22 speed ratio and 10% plate thickness reduction, increasing the stiffener reduction from 5 to 10% reduced the curvature from 0.00003 to − 0.00453 mm^{-1}. This is attributed to the further extension of the stiffener, which adds bending stresses in form of tension within it.

At r_p of 15% and $r_{stif.}$ of 5%, all k values remain positive across the studied speed ratio range, likely because the plate extended more than the stiffener due to applying higher reduction which leads the panel to bent upwards. This emphasises the importance of the reduction ratio δ_r between the stiffener and plate thickness in controlling the curvature

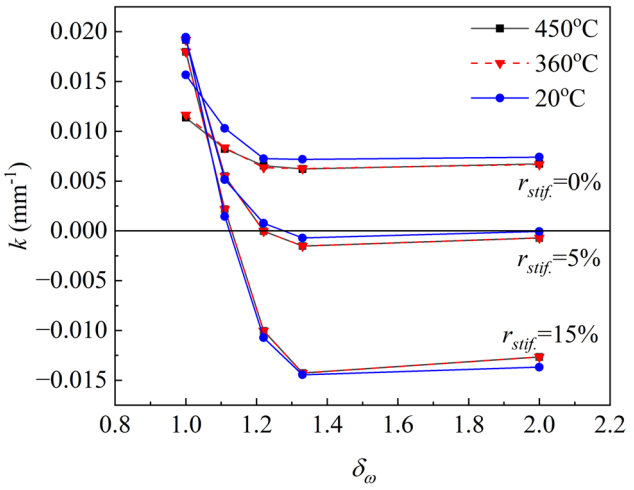

Fig. 10 The relationship between the curvature k and rotation speed ratio δ_ω at various stiffener reductions for different rolling temperatures of 20 ℃, 360 ℃, and 450 ℃. The invariant rolling conditions are AA6061, H_o = 3 mm, h_o = 10 mm, r_p = 10%, $D_1 = D_2$ = 100 mm, $\mu_1 = \mu_2$ = 0.8, ω_1 = 7.5 rpm

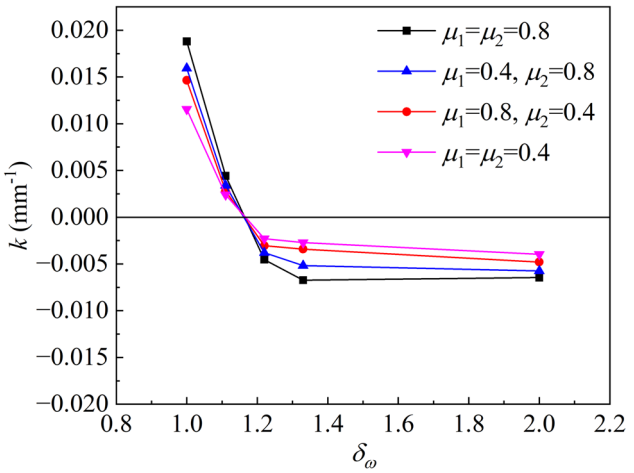

Fig. 11 The relationship between the curvature k and rotation speed ratio δ_ω for using different friction coefficients ranging from 0.4 to 0.8. The invariant rolling conditions are AA6061, T = 450 ℃, H_o = 3 mm, h_o = 10 mm, r_p = 10%, $r_{stif.}$ = 10%, $D_1 = D_2$ = 100 mm, ω_1 = 7.5 rpm

range. For example, the reduction ratio δ_r was 0.33 in this case, the lowest among the trends, which resulted in the highest k values. Conversely, with a plate thickness reduction of 5% and a stiffener reduction of 10%, the reduction ratio was 2, the highest value, corresponding to the lowest k values. Therefore, a low δ_r, such as 0.33 with r_p at 15%, makes producing a straight stiffened panel more challenging, even as the speed ratio increases. Conversely, applying a higher δ_r can help ensure the production of a straight stiffened panel with less dependence on the speed ratio.

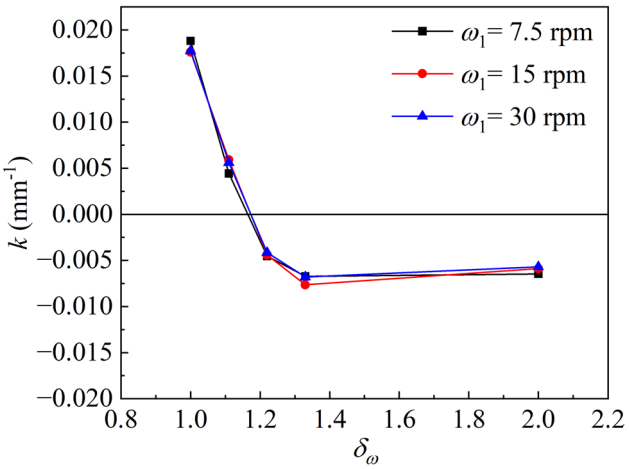

Fig. 12 The relationship between the curvature k and rotation speed ratio δ_ω using different rolling speeds at 7, 15, & 30 rpm. The invariant rolling conditions are AA6061, T = 450 ℃, H_o= 3 mm, h_o= 10 mm, r_p = 10%, $r_{stif.}$ = 10%, $D_1 = D_2$ = 100 mm, $\mu_1 = \mu_2$ = 0.8

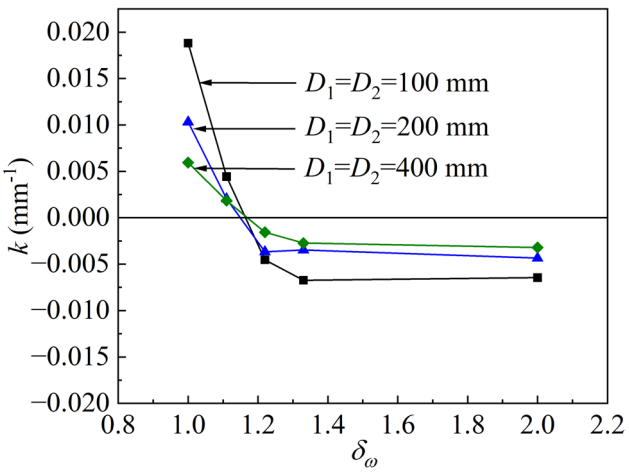

Fig. 13 The relationship between the curvature k and rotation speed ratio δ_ω using different roll diameters at 100, 200, and 400 mm. The invariant rolling conditions are AA6061, T = 450 ℃, H_o= 3 mm, h_o= 10 mm, r_p = 10%, $r_{stif.}$ = 10%, $\mu_1 = \mu_2$ = 0.8, ω_1= 7.5 rpm

b) Rolling temperatures ***T***

Figure 10 shows the evolution of the curvature k with the speed ratio δ_ω at different stiffener reductions. For each δ_ω, the effects of three rolling temperatures, i.e. 20 ℃, 360 ℃, and 450 ℃, are compared. The results for 360 ℃ and 450 ℃ are almost identical. Generally, the different rolling temperatures have no significant influence on the curvature profile, indicating that temperature is not a dominant factor influencing rolled panel curvature. However, rolling temperature is still a critical parameter in industrial rolling process since it can significantly affect the force required

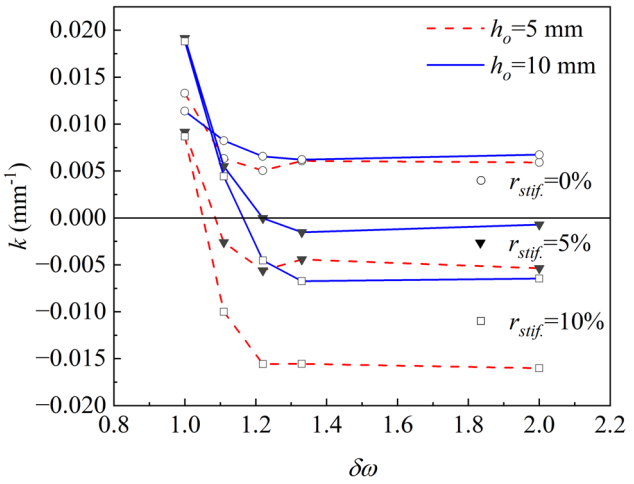

Fig. 14 The relationship between the curvature k and rotation speed ratio δ_ω using different stiffener heights h_o of 5 mm, and 10 mm. The invariant rolling conditions are AA6061, T = 450 ℃, H_o= 3 mm, r_p = 10%, $D_1 = D_2$ = 100 mm $\mu_1 = \mu_2$ = 0.8, ω_1 = 7.5 rpm

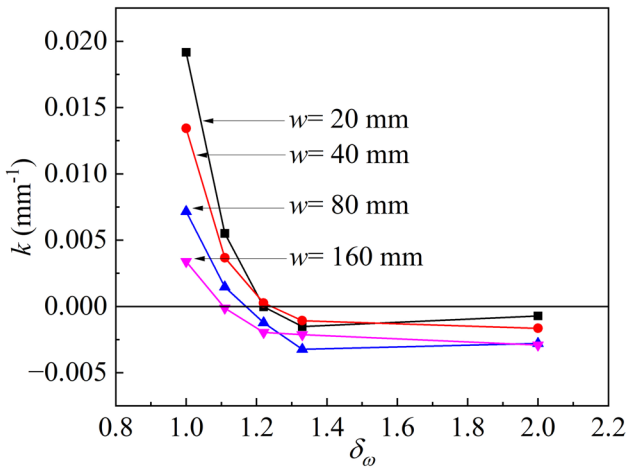

Fig. 15 The relationship between the curvature k and rotation speed ratio δ_ω using different plate width w of 20, 40, 80, and 160 mm. The invariant rolling conditions are AA6061, T = 450 ℃, H_o= 3 mm, h_o= 10 mm, r_p= 10%, $r_{stif.}$ = 10%,$D_1 = D_2$ = 100 mm, $\mu_1 = \mu_2$ = 0.8, ω_1 = 7.5 rpm

during rolling process, as well as the microstructural and mechanical properties of the material [36].

c) Friction coefficients $\boldsymbol{\mu}_1$, and $\boldsymbol{\mu}_2$

Figure 11 illustrates the variation of the curvature k against speed ratios δ_ω for different friction coefficients μ_1 and μ_2 applied to the lower and upper rolls, respectively. These correspond to various friction ratios ($\delta_\mu = \mu_2/\mu_1$), specifically 0.8/0.8, 0.8/0.4, 0.4/0.8, and 0.4/0.4. At the

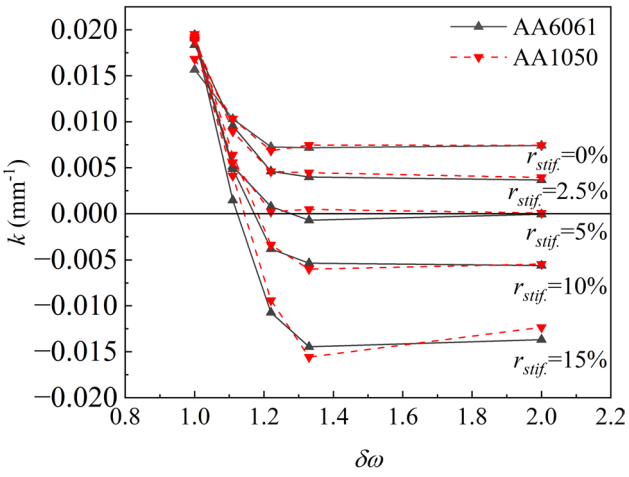

Fig. 16 The relationship between the curvature k and rotation speed ratio δ_ω using different rolled material of AA1050 and AA6061. The invariant rolling conditions are T = 20 ℃, H_o= 3 mm, h_o= 10 mm, r_p= 10%, $r_{stif.}$= 10%,$D_1 = D_2$ = 100 mm, $\mu_1 = \mu_2$ = 0.8, ω_1= 7.5 rpm

friction coefficient of μ_1 = 0.8 and μ_2= 0.8, within the studied speed ratio range, the maximum curvature is k = 0.019 mm^{-1}, while the minimum is k = −0.06 mm^{-1}. Reducing μ_1 from 0.8 to 0.4 narrows the overall range of k, as the maximum curvature decreases to k = 0.016 mm^{-1} and the minimum increases to k = −0.05 mm^{-1}. In addition, keeping μ_1 constant at 0.8 while lowering μ_2 to 0.4 results in further narrowing of the curvature range, suggesting that the curvature is more sensitive to changes in the friction coefficient of the lower roll compared to the upper roll. When both μ_1 and μ_2 are decreased to 0.4, the curvature range narrows even further, with a maximum of k = 0.012 mm^{-1} and a minimum of k = −0.03 mm^{-1}.

d) Rolling speeds $\boldsymbol{\omega}_1$

Figure 12 illustrates the variation of the curvature k against speed ratios δ_ω for different speeds ω_1 at 7.5, 15, and 30 rpm. Altering the rolling speeds seems to have minimal impact on the curvature, as all trends exhibit similar behaviour. However, variations in roll speed can marginally affect the curvature in indirect way. As roll speed increases, the temperature of the rolled stiffened panel also rises. This is due to the greater heat generated from plastic deformation combined with a reduced contact time for heat exchange between the hot stiffened panel and the cold rolls. This temperature increase may slightly influence the material properties of the rolled panel, thus affecting the curvature [37]. Additionally, higher roll speeds reduce the roll force [38], which may contribute to slightly differences in the curvature.

e) Roll diameter $\boldsymbol{D}_1$ and $\boldsymbol{D}_2$

Figure 13 illustrates the variation of curvature k versus speed ratios δ_ω for different roll diameters ($D_1 = D_2$). Three roll diameters were utilised: 100 mm, 200 mm, and 400 mm. Increasing the roll diameter narrows the range of k across different speed ratio. Specifically, the curvature exhibits greater sensitivity to speed ratio change with a smaller roll diameter, while it remains more stable with a larger one. At a speed ratio of 1, all rolled stiffened panels curved upward, almost wrapping around the upper roll surface. Consequently, the maximum k values that can be reached for each roll diameter (trend) for diameters of 100, 200, and 400 mm are approximately 0.02, 0.01, and 0.005 mm^{-1}, respectively, as $k = 1/R$. On the other hand, the minimum k values are approximately -0.07, -0.04, and -0.03 mm^{-1}, for diameters of 100, 200, and 400 mm, respectively. This results in a narrower range of k for the larger diameter of 400 mm, and a wider range for the smaller diameter of 100 mm. Thus, larger roll diameters lead to more stable curvature variation with less sensitivity to speed ratio changes, while smaller diameters allow for greater variability in curvature. This effect is reasonable because larger roll diameters induce less localised deformation on the rolled panel, as they engage a greater surface area during rolling. This broader surface engagement leads to more distributed deformation, resulting in less pronounced curvature.

f) Original stiffener hights $\boldsymbol{h_o}$

Figure 14 illustrates the variation of the curvature k against speed ratios δ_ω for stiffened panels with different stiffener heights h_o at 5 mm (red dashed line), and 10 mm (blue solid line), each at stiffener reductions of 0%, 5%, and 10%. Under certain rolling conditions, lower stiffener height of 5 mm results in a lower curvature compared with higher stiffener height of 10 mm. This suggests that, for achieving a straight stiffened panel at a given speed ratio, increasing the original stiffener height will need a corresponding increase in the stiffener reduction.

g) Plate widths $\boldsymbol{w}$

Figure 15 illustrates the impact of varying plate widths (w) at 20, 40, 80, and 160 mm, on the curvature with respect to the rotation speed ratio (δ_ω). Increasing the plate width leads to a reduction in the curvature, specifically within the speed ratio range up to 1.11 approximately. At a speed ratio of 1, rolling a stiffened panel with a width of 20 mm results in upward bending, characterised by a higher curvature. However, as the plate width increases, its moment of inertia also increases, enhancing the plate's resistance to bending. Consequently, wider plates exhibit a lower curvature. Nevertheless, at higher speed ratios from 1.33 to 2, the bending resistance reduces, resulting in a narrower variation in the curvature across all plate widths.

h) Rolled materials

Figure 16 illustrates the variation in curvature k with speed ratio δ_ω for two different aluminium alloys, AA6061 and AA1050. These alloys were selected due to their large difference in stress flow behaviour, which could influence the panel rolling performance. Similar simulation approach can be extended to a wide range of aluminium alloys. AA6061, known for its higher in strength and stiffness compared to AA1050, is generally more resistant to deformation during the rolling process. This resistance could potentially influence the curvature profile. However, as depicted in Fig. 16, no significant difference in the curvature was observed between the two materials. This suggests that the impact of changing the material is relatively minor compared to other rolling parameters, leading to similar curvature profiles despite the differences in material deformability.

i) Summary of parameters influencing panel curvature

The analysis of curvature variations in rolled panels, derived from 265 simulations, highlights the impact of different parameters on the curvature k, as summarised in Table 5. The successful production of a stiffened panel through a rolling process depends heavily on the careful adjustment of key parameters such as plate thickness reduction, stiffener reduction, and speed ratio, which have the most significant effects on the final curvature profile. While other parameters like roll diameter, friction, and rolling temperature, also influence the curvature, their effects are secondary compared to these primary parameters.

3.7 Key insights from simulation analysis for rolling experiments of stiffened panel

The following points summarise critical consideration of the key insights from simulation analysis for rolling experiments designed:

1) Keeping stiffener reduction equal to plate thickness reduction is appropriate in rolling test. According to FE result (Figs. 7 and 8), if stiffener reduction is less than the plate thickness reduction, the material deformation in stiffener is limited, causing gap between upper roll and stiffener, and hence bad geometry accuracy. Additionally, it will narrow the range of k, even unable to roll a straight panel whatever the speed ratio is (Figs. 6

Table 5 The effect of rolling parameters on the curvature variation

Rolling parameters	Effect on curvature k	Related figures
Stiffener reduction $r_{stif.}$	Increasing stiffener reduction leads to a decrease in k	Figures 9, 10, 11, 12, 13, 14, 15, 16
Speed ratio δ_ω	k decreases with increasing the δ_ω until reaching the minimum peak. Subsequent increases in δ_ω have diminishing effects	Figures 9, 10, 11, 12, 13, 14, 15, 16
Reduction of plate thickness r_p	Increasing r_p raises k	Figure 9
Rolling temperature T	No significant effect on k	Figure 10
Friction μ	High friction in both rolls increases the range of k	Figure 11
Speed ω	No significant effect on k	Figure 12
Diameter D	Increasing roll diameter decreases the range of k	Figure 13
Stiffener height h_o	Elevating the original stiffener height increases k	Figure 14
Plate width w	Increasing plate width reduces the k	Figure 15
Stiffened panel material	No significant effect on k	Figure 16

and 10). If stiffener reduction is greater than the plate thickness reduction, material flow from stiffener to plate, causing a localised distortion and stress concentration, hence bad geometry accuracy and roll life span. Therefore, stiffener reduction equal to the plate thickness reduction is suggested during the experiment design of rolling a stiffened panel.

2) A novel manufacturing process can be proposed to produce stiffened panels with good surface quality, high geometry accuracy, and either straight or curved shape. The procedure includes:
   a) Clarify the desired final geometry of stiffened panel, including cross-sectional dimensions and curvature.
   b) Design the cross-sectional geometry of semi-finished panel based on the given target geometry, ensuring equal reductions in the stiffener and plate. Manufacture the straight semi-finished stiffened panels preferably by extrusion.
   c) Determine appropriate rolling parameters, with focus on speed ratio and secondary factors such as roll diameter and rolling temperature through numerical simulations.
   d) Perform rolling tests, compare the results to simulations, and adjust the speed ratio as needed to achieve the desired curvature.
3) Since friction coefficient has limited effect on k, lubricant, particularly, in the groove of the roll, can be used in the real rolling test to avoid sticking.
4) Since material, speed, and temperature have limited effects on k, a unified set of rolling parameters (speed ratio, reductions) can be used for various materials under different temperatures and speeds, without influencing the rolled shape. Therefore, the rolling processing window of temperature and speed can be obtained to obtain panels with desired shape and microstructures.

4 Conclusions

This study analyzes finite element simulation results of rolling a stiffened panel, aiming to explore the influence of various rolling parameters, including reductions in plate thickness and stiffener cross-sectional area, speed ratio, roll diameter, friction coefficient, temperature, and material type on the curvature profile. These findings provide valuable insights for designing a novel and optimal rolling process for stiffened panels. The key conclusions in this study are drawn as follows:

1) The main rolling parameters influencing the final panel curvature are the reductions in the plate thickness and stiffener, as well as the speed ratio. Increasing the plate thickness reduction from 5 to 15% increased the curvature from − 0.01022 to 0.00178 mm^{-1} under the rolling conditions of 1.22 speed ratio and 10% stiffener reduction. At the same 1.22 speed ratio with 10% plate thickness reduction, increasing the stiffener reduction from 5 to 10% reduced the curvature from 0.00003 to − 0.00453 mm^{-1}. When the speed ratio transitions from 1.11 to 1.33 with a plate thickness reduction of 10% and a stiffener reduction of 10%, the curvature undergoes significant decrease from 0.004 to − 0.00656 mm^{-1}.
2) The roll diameter and friction coefficient have minor effect on the final panel curvature. Using larger diameters provide more stable outcomes of curvature variation. Since friction coefficient shows minor effect on the curvature. This suggests that lubricant can be used, especially in groove rolls, to avoid sticking without affecting the final panel shape.
3) Other variables like rolling temperature, roll speed, and panel material do not show significant effect on the curvature of the rolled stiffened panel.
4) Maintaining equal reductions in both plate and stiffener is recommended for the rolling process to help produc-

ing the most geometrically accurate panels, preventing material underfilling or overfilling of the groove.

Acknowledgements Authors appreciate the financial support and scholarship for Y. Alfawzan from King Abdulaziz City for Science and Technology (KACST), through Royal Embassy of Saudi Arabia Cultural Bureau (UKSACB) in the UK.

Author contribution All authors contributed to the study's conception and design. Methodology, data collection, and analysis were performed by Y. Alfawzan and J. Lv. The first draft of the manuscript was written by Y. Alfawzan, and all authors (J. Lv, Z. Shi, and J. Lin) commented on previous versions of the manuscript. All authors read and approved the final manuscript.

Declarations

Ethics approval Not applicable.

Consent to participate Not applicable.

Consent for publication Yes.

Competing interests The authors declare no competing interests.

References

1. Zha Y, Moan T (2001) Ultimate strength of stiffened aluminium panels with predominantly torsional failure modes. Thin-Walled Struct 39(8):631–648
2. Yao T, Fujikubo M (2016) Chapter 1 - introduction. In: T. Yao & M. Fujikubo (eds.) Buckling and ultimate strength of ship and ship-like floating structures. Butterworth-Heinemann, Oxford, pp 1–11. https://doi.org/10.1016/B978-0-12-803849-9.00001-0
3. Zhang Z, Zhou W, Shi Z, Lin J (2022) Advances on manufacture methods for wide lightweight aluminium stiffened panels. IOP Conf Ser: Mater Sci Eng 1270(1):012122
4. Pettit R, Wang J, Toh C (2000) Validated feasibility study of integrally stiffened metallic fuselage panels for reducing manufacturing costs. NASA Technical Reports Server. https://ntrs.nasa.gov/citations/20000057324. Accessed 20 June 2024
5. Murphy A, Lynch F, Price M, Gibson A (2006) Modified stiffened panel analysis methods for laser beam and friction stir welded aircraft panels. Proc Inst Mech Eng, Part G: J Aerosp Eng 220(4):267–278
6. Rajendran C, Srinivasan K, Balasubramanian V, Balaji H, Selvaraj P (2019) Evaluation of load-carrying capabilities of friction stir welded, tig welded and riveted joints of aa2014-t6 aluminium alloy. Aircr Eng Aerosp Technol 91(9):1238–1244
7. Moreira PMGP, Richter-Trummer V, de Castro PMST (2012) Lightweight stiffened panels fabricated using emerging fabrication technologies: fatigue behaviour. in Structural connections for lightweight metallic structures. Springer Berlin Heidelberg, Berlin, Heidelberg, pp 151–172
8. Li B, Gao H, Deng H, Wang C (2020) A machining deformation control method of thin-walled part based on enhancing the equivalent bending stiffness. Int J Adv Manuf Technol 108:2775–2790
9. Munroe J, Wilkins K, Gruber M, Domack M (2000) Integral Airframe Structures (IAS): validated feasibility study of integrally stiffened metallic fuselage panels for reducing manufacturing costs, Secondary. NASA: Long Beach, California
10. Zhang Z, Zhou W, Shi Z, Lin J (2023) Investigation of die designs on welding quality and billet material utilisation for multi-container extrusion of wide stiffened aluminium panels. Int J Adv Manuf Technol 127(9):4149–4162
11. Lv J, Yu J, Shi Z, Li W, Lin J (2023) Feasibility study of a novel multi-container extrusion method for manufacturing wide aluminium profiles with low force. J Manuf Process 85:584–593
12. Alfawzan Y, Shi Z, Lin J (2022) Development and perspectives of rolling of rib stiffened plate. IOP Conf Ser: Mater Sci Eng 1270(1):012058
13. Kraner J et al (2020) A review of asymmetric rolling. Materiali in tehnologije 54:731–743
14. Pan D, Sansome DH (1982) An experimental study of the effect of roll-speed mismatch on the rolling load during the cold rolling of thin strip. J Mech Work Technol 6(4):361–377
15. Pustovoytov D, Pesin A, Tandon P (2021) Asymmetric (hot, warm, cold, cryo) rolling of light alloys: a review. Metals 11(6):956
16. Ji Y, Park J (2009) Development of severe plastic deformation by various asymmetric rolling processes. Mater Sci Eng, A 499(1–2):14–17
17. Johnson W, Needham G (1966) Further experiments in asymmetrical rolling. Int J Mech Sci 8(6):443–455
18. Aboutorabi A, Assempour A, Afrasiab H (2016) Analytical approach for calculating the sheet output curvature in asymmetrical rolling: In the case of roll axis displacement as a new asymmetry factor. Int J Mech Sci 105:11–22
19. Dewhurst P, Collins IF, Johnson W (1974) A theoretical and experimental investigation into asymmetrical hot rolling. Int J Mech Sci 16(6):389–397
20. Shivpuri R, Chou P, Lau C (1988) Finite element investigation of curling in non-symmetric rolling of flat stock. Int J Mech Sci 30(9):625–635
21. Knight CW, Hardy SJ, Lees AW, Brown KJ (2003) Investigations into the influence of asymmetric factors and rolling parameters on strip curvature during hot rolling. J Mater Process Technol 134(2):180–189
22. Salimi M, Sassani F (2002) Modified slab analysis of asymmetrical plate rolling. Int J Mech Sci 44(9):1999–2023
23. Buxton S, Browning S (1972) Turn-up and turn-down in hot rolling: a study on a model mill using plasticine. J Mech Eng Sci 14(4):245–254
24. Knight CW, Hardy SJ, Lees AW, Brown KJ (2005) Influence of roll speed mismatch on strip curvature during the roughing stages of a hot rolling mill. J Mater Process Technol 168(1):184–188
25. Qwamizadeh M, Kadkhodaei M, Salimi M (2012) Asymmetrical sheet rolling analysis and evaluation of developed curvature. Int J Adv Manuf Technol 61(1):227–235
26. Jeswiet J, Greene PG (1998) Experimental measurement of curl in rolling. J Mater Process Technol 84(1):202–209

27. Fu Y, Xie S, Xiong B, Huang G, Cheng L (2012) Effect of rolling parameters on plate curvature during snake rolling. J Wuhan Univ Technology-Mater Sci Ed 27:247–251
28. Collins IF, Dewhurst P (1975) A slipline field analysis of asymmetrical hot rolling. Int J Mech Sci 17(10):643–651
29. Lu JS, Harrer OK, Schwenzfeier W, Fischer FD (2000) Analysis of the bending of the rolling material in asymmetrical sheet rolling. Int J Mech Sci 42(1):49–61
30. Minton J, Brambley E (2017) Meta-analysis of curvature trends in asymmetric rolling. Procedia Eng 207:1355–1360
31. Na DH, Cho SH, Lee Y (2011) Experimental and numerical studies for the forming groove and separating groove design in slit rolling process. J Mech Sci Technol 25(9):2439–2446
32. IspatGuru (2014) Roll pass design. https://www.ispatguru.com/roll-pass-design/. Accessed 15 June 2022
33. Zaharoff TL, Johnson RE, Karabin ME (1992) Spread in sheet rolling: a comparison using experiments, analytical solutions and numerical techniques. Int J Mech Sci 34(6):435–442
34. Biba N, Stebunov S, Vlasov A (2017) Material forming simulation environment based on qform3d software system. Energy 2:4
35. Equation of a circle passing through 3 given points. https://planetcalc.com/8116/. Accessed 01 Feb 2023
36. Rajabi F, Zarei-Hanzaki A, Eskandari M, Khoddam S (2013) The effects of rolling parameters on the mechanical behavior of 6061 aluminum alloy. Mater Sci Eng, A 578:90–95
37. Galantucci LM, Tricarico L (1999) Thermo-mechanical simulation of a rolling process with an fem approach. J Mater Process Technol 92–93:494–501
38. Devarajan K, Marimuthu KP, Ramesh A (2012) Fem analysis of effect of rolling parameters on cold rolling process. Bonfring Int J Indust Eng Manage Sci 2(1):35